Proceedings of the 10th Brazilian Congress of Thermal Sciences and Engineering – ENCIT 2004
Braz. Soc. of Mechanical Sciences and Engineering – ABCM, Rio de Janeiro, Brazil, Nov. 29 – Dec. 03, 2004

Paper CIT04-0083

NUMERICAL STUDY OF THE FLOWFIELD STRUCTURES DURING THERMAL SPALLATION DRILLING PROCESS

Luís Fernando Figueira da Silva, Angela O. Nieckele, Fernanda M. C. Salgado
Department of Mechanical Engineering
Pontifícia Universidade Católica do Rio de Janeiro
Rua Marquês de São Vicente, 225
22453-900 Rio de Janeiro, RJ, BRAZIL
e-mail luisfer@mec.puc-rio.br, nieckele@mec.puc-rio.br, nandasalgado@yahoo.com.br

João Carlos Ribeiro Plácido
CENPES/PDEP/TEP
Cidade Universitária, Quadra 7
21949-900 Rio de Janeiro, RJ, BRAZIL
jcrp@cenpes.petrobras.com.br

Abstract. *Thermal spallation drilling is an excavation technique aimed at perforating hard rocks at high rates. In this technique a stream of dense supersonic gases issued from a combustion process impacts the rock. The high heat transfer rate is responsible for the dilatation of the exposed rock surface which leads to the opening and subsequent coalescence of the natural flaws which exist in the material. Once a critical flaw is formed, a spall is created and separated from the surface. Thus, fresh rock surface is exposed to the hot gases. This process leads to a progressive penetration of the rock surface. The prediction of the drilling rates requires the knowledge of thermo-mechanical rock properties and also of the physico-chemical processes involved in the flowfield. Indeed, the aforementioned interaction leads to a complex compressible flowfield with shear and boundary layers regions as well as large eddies carrying energy. This work investigates the flowfield structures present when a dense supersonic jet interacts with cavities of given shape. Different prescribed cavity geometries are studied, for each of them several flow parameters are varied. In particular, the influence of the pressure ratio between the dense jet and the cavity interior, and of the distance between the jet exit and the rock surface on the rock surface conditions are studied. To this end, a numerical code is used which solves the governing equations of mass, momentum and energy for two-dimensional axisymmetric configurations for a compressible mixture of perfect gases. These equations are discretized by a finite volume technique on unstructured meshes.*

keywords: *Supersonic flow, jets, compressibility*

1. Introduction

The technique dubbed thermal spallation drilling has been considered during the 1980's as a way of penetrating hard rocks in depths of several kilometers with the aim of producing geothermal energy (Williams et al., 1988). As schematically shown in Fig. 1, in this technique a dense supersonic jet, produced by a high pressure combustion process, interacts with the exposed face of the rock surface. The result of such an interaction is the progressive perforation of the rock. Since contact is avoided between the burner nozzle and the rock surface, the drilling tool is submitted to reduced wear, when compared to traditional rotary drilling equipment. This technique has also been used for drilling small holes in iron ore mining for the placement of explosive charges (Williams et al., 1988; Rauenzahn, 1986). However, not until recently the underlying physical mechanism leading to the rock breakup during thermal spallation drilling has been understood. Indeed, as shown in Fig. 2, the intense heat flux, which results from the interaction between the supersonic jet and the rock surface, leads to the buildup of compressive stresses in the vicinity of the region exposed to the hot gases. These stresses provoke the opening and coalescence of the flaws, which naturally occur within the material, in a direction parallel to the exposed surface. Once a flaw of critical dimension is formed, the buckling of the surface layer seems to occur and a spall is formed. The spall is then separated from the rock matrix and swept away by the gas flow, thus exposing a new rock layer to the intense heat flux. Since the thermal spallation mechanism involves rapid heating and breakup of a very small portion of the rock, it can be expected that the rocks which are more suitable to this penetration technique are hard fragile rocks possessing large thermal diffusivity and

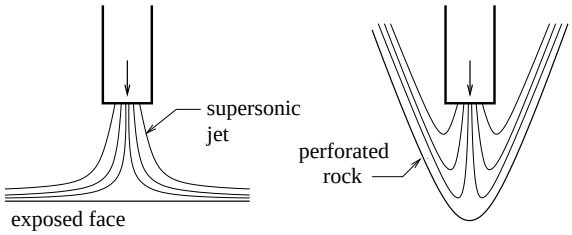

Figure 1: Schematic illustration of the thermal spallation drilling technique (Wilkinson and Tester, 1993).

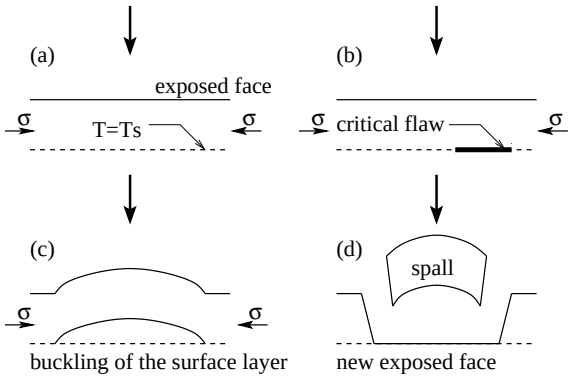

Figure 2: Illustration of the fracture mechanism leading to rock spallation (Wilkinson and Tester, 1993).

linear expansion coefficient. Indeed, this technique has been successfully applied to create boreholes in granite (Rauenzahn, 1986; Rauenzahn and Tester, 1991b). One should note that increasing the jet temperature until the rock melts is not energy efficient, since extra energy is required in the phase change process, and the layer of molten rock is harder to displace than the spalls.

Experimental studies used a rocket-engine type combustor, burning methane or propane with either air or oxygen, and led to heat fluxes of the order of 1 MW/cm^2 (Wilkinson, 1989; Wilkinson and Tester, 1993). Drilling velocities up to 10 meters per hour were obtained in granite, to an excavated depth of 300 meters. The diameter of the borehole perforated, around 30 cm, is 10 to 20 times larger than the nozzle exit diameter. Concerning the operating costs, it should be noted that, while the classical rotary rock drilling techniques involves costs which evolve exponentially with depth, thermal spallation drilling costs vary linearly with penetration depth (Tester et al., 1994). More recently, efforts have been concentrated in developing this technique to drill natural gas reservoirs. Also, recent experimental work (Viegas, 2004) shows successful perforation of both granites and carbonates.

Numerical studies of this drilling technique have developed a model for the interaction between the supersonic turbulent gases and the receding rock surface (Rauenzahn and Tester, 1991a; Wilkinson, 1989). However, little attention has been given to the effect of the choice of the hot jet parameters on the resulting flowfield, which is essential to the prediction of drilling rates.

2. Aerothermodynamical phenomenology

Several physical phenomena are tightly coupled during the thermal spallation drilling process:

- turbulent, unsteady, supersonic and subsonic compressible flows,
- radiation and convection heat transfer between the hot burned gases and the rock surface,
- interaction between the rock spalls and the flowfield.

The complete modeling of these phenomena is an open problem, the main difficulties associated with such modeling are discussed now.

Recent studies of supersonic hot and dense jets (Panda, 1998; Wu et al., 1999) have shown that, even in the absence of solid obstacles, high amplitude transverse oscillations are observed, which involve important pressure fluctuations. These oscillations, which are responsible for an increased mixing between the jet and the

surroundings, are found to be connected to the shock waves present in the flowfield. As shown in Fig. 1, the presence of a solid obstacle substantially modifies the flow. Besides from decelerating and deflecting the flow, the obstacle may have an amplification effect on longitudinal acoustic instabilities (Glaznev, 1991; Sokolov, 1992; Gorshkov et al., 1993; Gorshkov and Uskov, 1999). The overpressure induced by these oscillations may have characteristic frequencies of the order of several kilohertz and amplitudes of dozens of decibels. Both the frequency and the amplitude are found to be functions of the distance that separates the jet exit from the obstacle, also known as standoff distance, of the pressure ratio between the jet and the ambient air, and of the jet Mach number.

As far as turbulence modeling is concerned, the compressibility effects influence turbulent fluctuations both within the jet and on the boundary layer that develops over the rock surface. As opposed to low velocity flows, pressure fluctuations which occur in supersonic flows exert an important influence on the turbulence characteristics (Sarkar, 1995; Sarkar et al., 1991a; Sarkar et al., 1991b; Sakar and So, 1997), and, in particular, on the pressure-dilatation correlation and on the turbulent kinetic energy dissipation rate, which are found to be increasing functions of the turbulent Mach number. The boundary layer that develops over the rock surface is also modified by compressibility effects (Zeman, 1993; Zhang et al., 1991; Adumitroaie et al., 1998). Since the turbulent transport within the boundary layer is influenced by the aerodynamical compressibility, convective heat transfer between the gas and the rock surface is also modified.

Hydrocarbon combustion products often contain an important content of microscopic solid particles (Glassman, 1996). Since the temperature of these particles is close to those of the hot burned gases, the radiation heat flux between the flow and the rock surface which may be of the same order of magnitude as the convection heat transfer. Both these contributions should be accounted for when calculating the total heat flux, and thus the surface regression rate. The radiation heat transfer may be decreased by using gaseous fuels and by operating at either fuel lean or stoichiometric conditions. However, this may not be desirable from and efficiency standpoint.

The ejection of solid particles, whose diameter tipically lie between 1 and 10 mm (Wilkinson and Tester, 1993), by the spallation process should also influence the aerodynamic of the flowfield. In particular, the aerodynamic drag of the spalls, which may have velocities substantially different from the local gas velocity, may alter the turbulence characteristics and, consequently, the convective heat flux between the rock and the gas.

3. Mathematical formulation of the problem

In present case, the flowfield is simulated using the two-dimensional Navier-Stokes equations for a complex gas mixture, which can be written in the integral conservative form as

$$\iint_V \frac{\partial \boldsymbol{U}}{\partial t} y dx dy + \int_S (\boldsymbol{F} y dy - \boldsymbol{G} y dx) + \int_V \boldsymbol{H} y dx dy = 0\,. \tag{1}$$

The vector of conserved quantities, $\boldsymbol{U}$, the expressions for the convective flux vectors, $\boldsymbol{F}$ and $\boldsymbol{G}$, in the longitudinal (x) and radial (y) directions, respectively, are written as

$$\boldsymbol{U} = \begin{bmatrix} \rho \\ \rho u \\ \rho v \\ \rho E \\ \rho Y_1 \\ \rho Y_2 \\ \vdots \\ \rho Y_{N-1} \end{bmatrix}, \quad \boldsymbol{F} = \begin{bmatrix} \rho u \\ \rho u^2 + p - \tau_{xx} \\ \rho uv - \tau_{xy} \\ u(\rho E + p) - \Omega_y \\ \rho Y_1 (u + V_{x_1}) \\ \rho Y_2 (u + V_{x_2}) \\ \vdots \\ \rho Y_{N-1} (u + V_{x_{N-1}}) \end{bmatrix}, \quad \boldsymbol{G} = \begin{bmatrix} \rho v \\ \rho uv - \tau_{xy} \\ \rho v^2 + p - \tau_{yy} \\ v(\rho E + p) - \Omega_y \\ \rho Y_1 (v + V_{y_1}) \\ \rho Y_2 (v + V_{y_2}) \\ \vdots \\ \rho Y_{N-1} (v + V_{y_{N-1}}) \end{bmatrix}, \quad \boldsymbol{H} = \begin{bmatrix} 0 \\ 0 \\ -p/y \\ 0 \\ 0 \\ 0 \\ \vdots \\ 0 \end{bmatrix}. \tag{2}$$

The nomenclature used in this system of equations is the one usually adopted in aerospace applications, such that ρ is the density, u and v are the Cartesian velocity components, E is the total energy per unit of mass, Y_i is the mass fraction of the i-th species, and p is the static pressure. The viscous stresses τ_{xx}, τ_{xy}, τ_{yy} and the heat fluxes Ω_x and Ω_y are given by

$$\tau_{xx} = 2\mu \frac{\partial u}{\partial x} - \frac{2}{3}\mu \left(\frac{\partial u}{\partial x} + \frac{\partial v}{\partial y} \right), \tag{3}$$

$$\tau_{xy} = \mu \left(\frac{\partial u}{\partial y} + \frac{\partial v}{\partial x} \right), \tag{4}$$

$$\tau_{yy} = 2\mu\frac{\partial v}{\partial y} - \frac{2}{3}\mu\left(\frac{\partial u}{\partial x} + \frac{\partial v}{\partial y}\right), \tag{5}$$

$$\Omega_x = u\tau_{xx} + v\tau_{xy} + \lambda\frac{\partial T}{\partial x} - \rho\sum_{k=1}^{N} h_k Y_k V_{x_k}, \tag{6}$$

$$\Omega_y = u\tau_{xy} + v\tau_{yy} + \lambda\frac{\partial T}{\partial y} - \rho\sum_{k=1}^{N} h_k Y_k V_{y_k}, \tag{7}$$

where μ and λ are the mixture viscosity and thermal conductivity, and V_{x_k} and V_{y_k} are the diffusion velocities of species k in the directions x and y, given by Fick's law (Williams, 1985).

In the solution of the equation system (1), $N-1$ chemical species are necessary, since the mass fraction of the last chemical species, Y_N, is calculated as $Y_N = 1 - \sum_{i=1}^{N-1} Y_i$. The state equation for a mixture of thermally perfect gases,

$$p = \rho\mathcal{R}T\sum_{i=1}^{N}\frac{Y_i}{W_i}, \tag{8}$$

is used to evaluate the pressure, p. In this equation, T is the temperature, $\mathcal{R}$ is the universal gas constant and W_i is the molecular weight of species i. The total energy, E, is defined as the sum of the internal energy, e, and the kinetic energy,

$$E = e + \frac{1}{2}\left(u^2+v^2\right) = \sum_{i=1}^{N} Y_i e_i + \frac{1}{2}\left(u^2+v^2\right) = \sum_{i=1}^{N} Y_i h_i - \frac{p}{\rho} + \frac{1}{2}\left(u^2+v^2\right). \tag{9}$$

The internal energy is a function of the mixture composition and of the temperature, T, which is calculated by a Newton method once e is known.

Note that the formulation above is used since it allows for temperature and composition dependent specific heats and transport properties, as well as variable composition of the burned gases (Figueira da Silva et al., 2000; Pimentel et al., 2002). The thermodynamic and transport properties are computed using Chemkin-II subroutines and databases (Kee et al., 1991; Kee et al., 1986)

4. Numerical method of solution

Computations are performed using a numerical code (Figueira da Silva et al., 1999; Figueira da Silva et al., 2000) that solves the governing equation system (1-2) using an upwind cell-centered finite volume method on unstructured triangular meshes. Temporal discretization uses a classical, 2nd-order, Runge-Kutta time stepping scheme (Mavriplis, 1988). In the spatial discretization, the interface fluxes are formulated using the Advection Upstream Splitting Method (AUSM$^+$, Liou, 1996). Spatial second order accuracy is sought with MUSCL (Hirsch, 1990) extrapolation.

5. Results and discussion

5.1. Calculation domain, initial and boundary conditions

In this study three fixed geometries are considered for the calculation domain. These geometries are shown in Fig. 3 (a). The difference between them is the shape of the surface of the rock being attacked by the flow of hot gases. The chosen forms are a plane, a sphere and an ellipse. The radius of the burner exit hole, 1 mm, and its external diameter, 10 mm are fixed. These dimensions are chosen in accordance to the experimental setup developed in parallel with the present numerical study (Viegas, 2004). The diameter of the perforated hole, 30 mm, is also kept constant. Two values are considered for the distance between the burner exit and the point of impact of the jet along the symmetry axis (x), 15 and 30 mm, this distance is also referred to as the standoff distance.

In Fig. 3 (a) are indicated the boundary conditions used. The walls are considered adiabatic and non catalytic, a spallation model for the regression rate due to the process of thermal spallation is not included. The nozzle is also considered to be an adiabatic, non catalytic, surface. At the entrance of the calculation domain

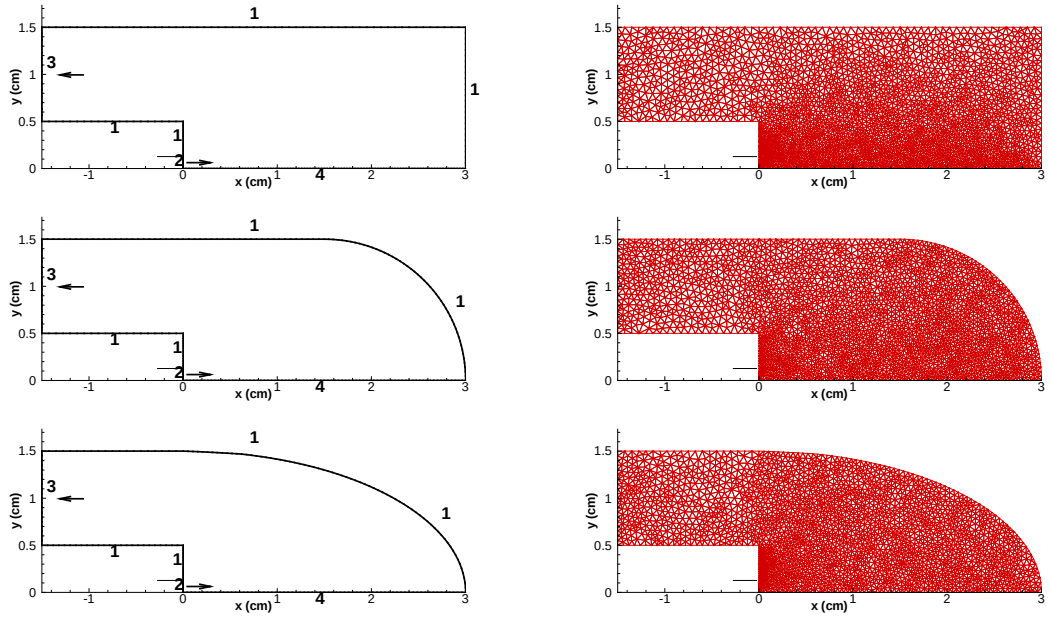

(a) Computational domain and boundary conditions

(b) Computational Meshes

Figure 3: Computational domains, boundary conditions and meshes used: (1) wall, (2) entrance, (3) exit, and (4) symmetry.

the flow is supersonic and parallel to the symmetry axis, with fixed Mach number ($M = 2$), static temperature ($T_{in} = 2850$ K) and static pressure ($P_{in} = 1$ atm). The composition of the jet corresponds to the main products of combustion of a stoichiometric, natural gas/oxygen mixture, i.e., CO_2, H_2O, CO, OH (13.7/53.7/20.0/12.6) in volume. Note that this composition is frozen throughout the computational domain. Considering either equilibrium of finite rate kinetics of the combustion would lead to smaller temperatures at stagnation regions of the flow due to increased dissociation.

At the exit boundary a simple extrapolation of the flow properties is used. Concerning the initial conditions prevailing at the computational domain, except for the exit nozzle of the burned gases, the gas is initially at rest. At the whole computational domain, the initial mixture composition and the static temperature are identical to those of the hot gases leaving the nozzle. In this study several values of static pressure for the gas that is initially at rest are considered, $p_{ext} = 0.5$, 0.9, 1.1 and 2.0 atm.

Concerning the computational meshes adopted, the domain of calculation is discretized using triangular meshes, as shown in Fig. 3 (b). The boundary elements of the different geometries maintained intervals of same dimension. The number of resulting computational volumes is 6122, 5863 and 5199 respectively. Although a study of the sensitivity of the obtained result on the number of triangles in the mesh has not been made, it is believed, based on previous experience (Figueira da Silva et al., 2000), that the chosen discretization is sufficient to capture the overall flow structures present.

5.2. Description of the overall flow structure

Figure 4 (a) shows the evolution, starting from the beginning of the computation, of the temperature field inside the cavity in four instants, for the case of an ellipsoidal cavity and an external pressure of 0.5 atm. The total simulated time is of 4.5 ms. In this figure, it is possible to observe the formation of the supersonic jet, where the classical shock waves and expansion diamond patterns (Shapiro, 1983) are clearly seen. This is characteristic of under expanded supersonic jets, i.e., in which the pressure is initially superior to the ambient pressure. This jet is slowed down and deviated by the impact with the rock wall, creating an area of high temperature on the rock surface close to the symmetry axis. It is observed that the temperature at the surroundings of the rock surface, close to the jet center, does not vary considerably once past the initial transient of the impact between the jet and the rock. The stagnation point corresponds to the maximum values of temperature and

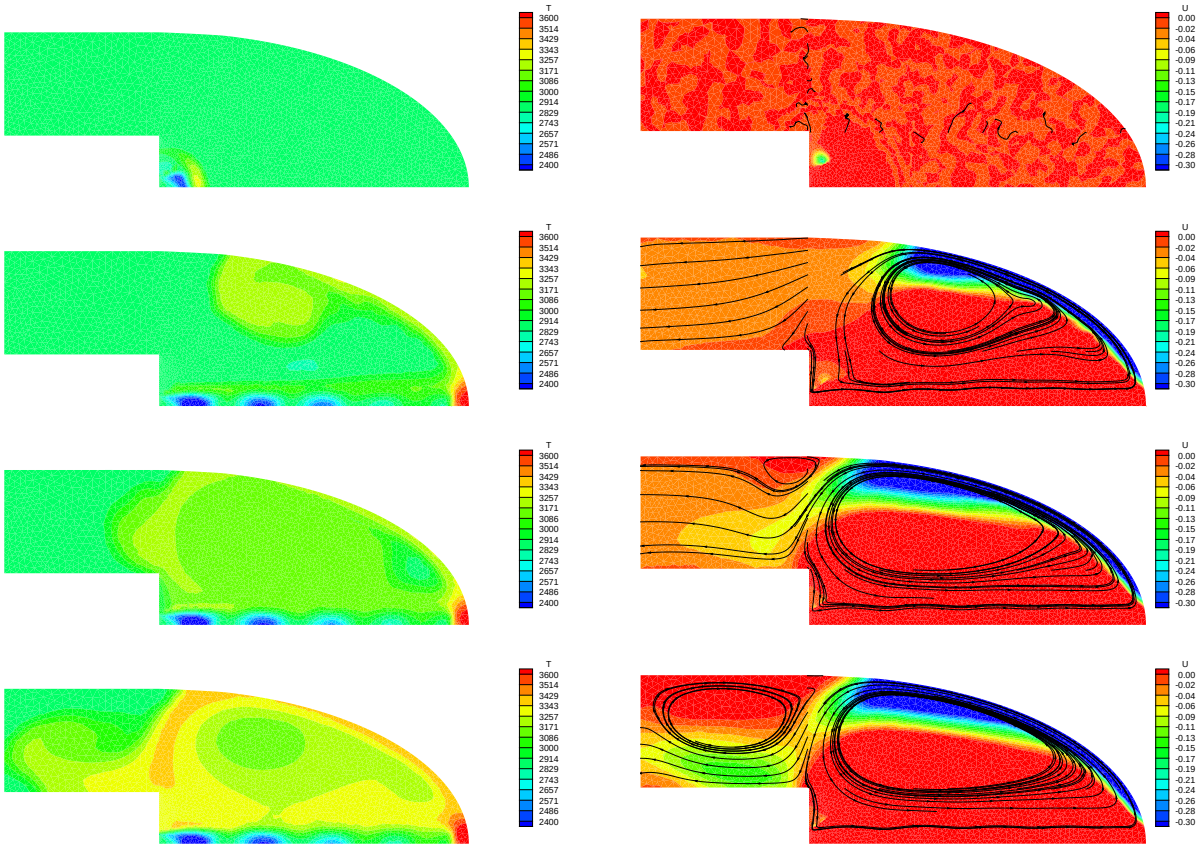

(a) Temperature

(b) Longitudinal velocity

Figure 4: Evolutions inside the cavity for different, equally spaced, time intervals, (a) temperature (K) and (b) longitudinal velocity and streamlines, for $p_{in} = 1$ atm and $p_{ext} = 0.5$ atm.

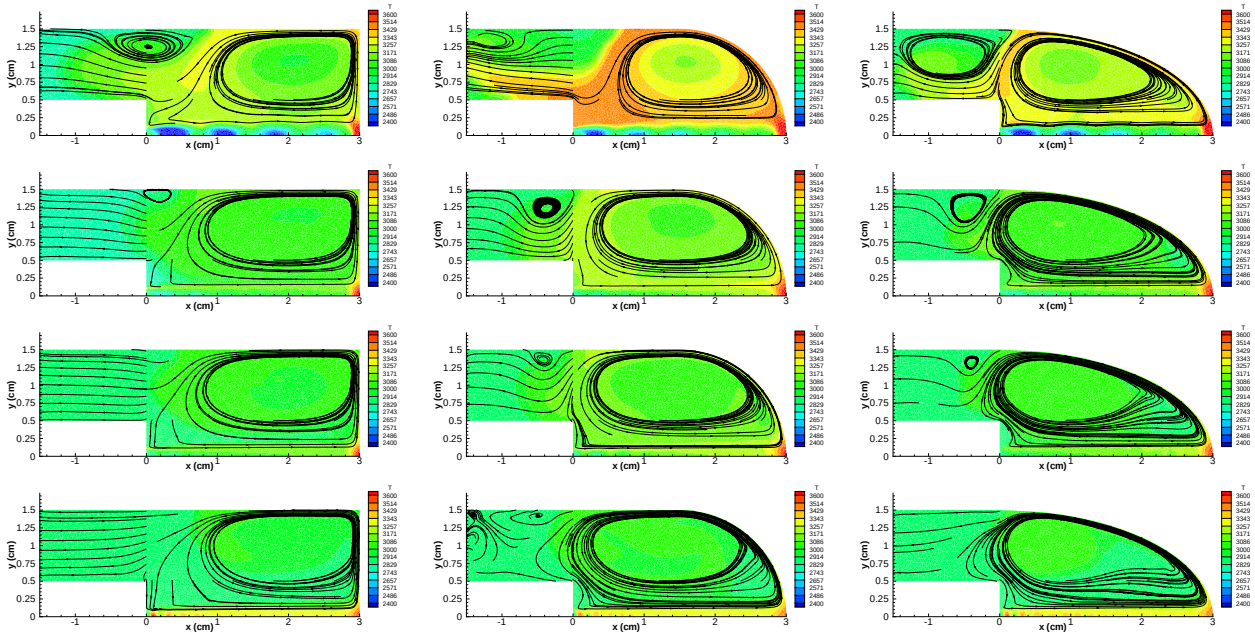

Figure 5: Comparison between the temperature fields and Eulerian streamlines obtained for different prescribed geometries and for different cavity to jet pressure ratios: 0.5, 0.9, 1.1 and 2.0 (from top to bottom). The temperature range spans from 2400 to 3600 K, with 286 K intervals.

pressure in the flow. Aerodynamic resonance effects, that will be detailed further on, are observed, however, in most simulated cases, the amplitudes of pressure and temperature fluctuations are small, when compared to the averaged levels. The jet deviation by the rock wall is followed by the formation of an area of recirculation of hot gases, which can be better visualized by the streamlines shown in Fig. 4 (b).

The recirculation zone, that can be clearly seen in Fig. 4 (b), lies between the cavity walls and the burner body, having as fluid limits the supersonic jet and the suction area located between the burner body and the cavity wall. Once formed, the dimension of this zone is practically constant during the simulation. It should be noted, however, that a pulsation of small amplitude of the dimension of this zone is observed. The presence of this first recirculation zone induces the formation of a secondary recirculation that, unlike the previous one, is not stable. As this secondary recirculation size increases, it is displaced by the flow toward the exit of the computational domain. When this zone reaches the exit of the domain, the boundary conditions adopted are not valid anymore, since part of the flow comes from the exterior to the interior of the calculation domain. Results where the total calculation time is increased showed that the formation of this zone of secondary recirculation occurs in a periodic way. However, a rigorous analysis of this phenomenon requires more extensive calculation domains than those adopted here, as well as a more realistic description of the exit boundary condition.

5.3. Influence of the geometry of the hole on the flow structure

In Fig. 5 are compared the temperature fields and the Eulerian streamlines obtained after stabilization of the primary recirculation zone, for the different chosen cavity geometries, and four values of pressure ratio between the jet and the exterior. For all of the chosen cavity geometries, an increase of the pressure ratio between the exterior and the jet leads to a decrease in the size of the zone of secondary recirculation. This occurs simultaneously with a rapid increase of the zone of primary recirculation. For the largest values of external pressure, the secondary zone is not observed. The causes of the disappearance of this recirculation zone were not investigated. However, it may be expected that, for larger values of the pressure ratio between the jet and the exterior, a larger amount of external gas is put in movement by the effect of the jet suction. Indeed, the momentum of the supersonic jet is responsible for the negative transverse velocities close to the burner rim. This figure also shows that, for a given ratio of pressures, a decrease of the cavity volume leads to a small increase in the size of the primary recirculation.

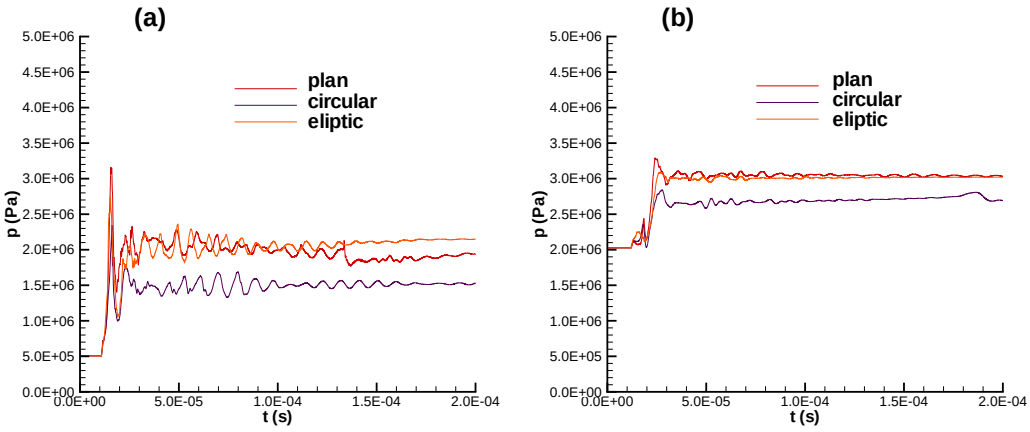

Figure 6: Pressure (Pa) history at the stagnation point for different cavity shapes and two values of the cavity initial pressure, p_{ext}, (a) 0.5 atm, (b) 2.0 atm.

5.4. Influence of the jet pressure and of the standoff distance

As it was observed previously, at the jet impact point on the symmetry line, the temperature and pressure conditions are the most severe. Therefore, it is expected the largest regression rate of the rock surface at this point. However, a parametric study of the regression rate of the rock surface requires a model for the process of thermal spallation, which is out of the scope of this work. It is of interest here the study of the physical parameters that lead to a steady state of the flow. To this end, it is shown in Fig. 6 the time evolution of the pressure at the point of central impact of the jet on the surface of the rock, for different hole shapes and for two cavity pressure values. For the depicted cases, after an initial transient, the pressure is stabilized in a value that seems to depend on the form of the cavity. In the case with larger initial external pressure, for which the supersonic jet is overexpanded with respect to the gas present in the cavity, the initial transient is quickly weakened. In the case where the exit pressure of the jet is larger than the existent in the cavity, important pressure variations are observed, in which the amplitude can reach 10% of the average value, before the steady state is reached. In the cases shown in Fig. 6, these oscillations are progressively dampened, until the pressure value reaches a plateau. It should be noted that other flow properties, as the temperature and density, presented similar oscillations.

The results shown in Fig. 7 allow to verify that a damping of the pressure oscillations does not always occurs. In this figure the pressure evolutions are compared in the bottom of a plane cavity, for two distances between jet and wall and four values of the initial pressure. This figure shows that, the smaller the distance between the jet exit and the bottom of the cavity, the larger the value of the pressure at the jet impact point. For the cases of smallest distance between the jet exit and the wall, 15 mm, undampened, periodic, pressure oscillations appear. In the case corresponding to the largest value of the external pressure (2.0 atm), the over pressure caused by such oscillations is insignificant. In the case where the jet is underexpanded, the pressure oscillations that are observed reach 15% of the average value of the pressure. In this case, the oscillation frequency is constant and equal to 500 kHz.

Although the mechanism responsible for the presence of a characteristic frequency needs to be investigated, a first exam of the time evolution of the flow suggests the existence of an acoustic coupling involving fluctuations in the shear layer existent at the jet periphery. These fluctuations may lead to oscillations in the longitudinal position of the normal shock wave located at the vicinity of the wall, which affects the pressure prevailing on the cavity bottom. These oscillations, which bear a clear ressemblance to those described in section 2, seem to have gone unnoticed in previous thermal spallation works. Whether these oscillations could benefit or hamper the perforation process remains an open question.

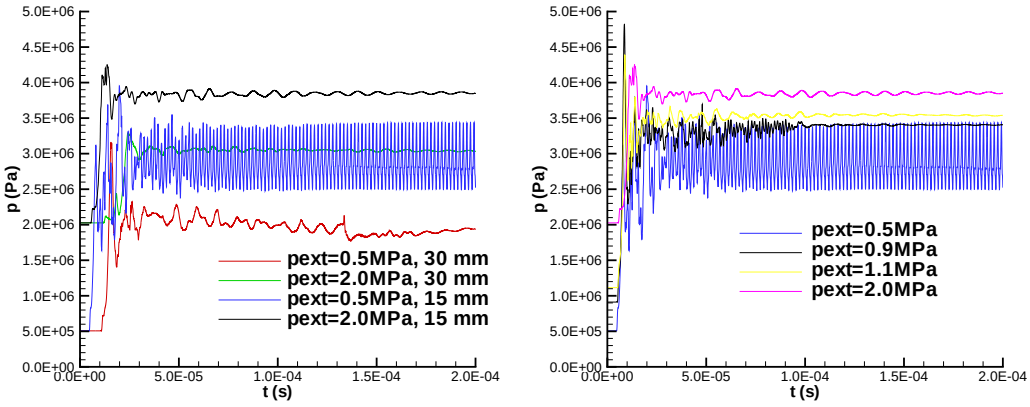

Figure 7: Pressure (Pa) history at the downhole stagnation point for (a) two values of the standoff distances and two values of the cavity initial pressure, (b) for a standoff distance of 15 mm and $p_{ext} = 0.5$ atm.

6. Acknowledgements

During this work L. F. Figueira da Silva was on leave from *Laboratoire de Combustion et de Détonique, Centre Nacional de la Recherche Scientifique*, France, with a PROFIX scholarship from CNPq-Brazil. Financial support for the present research was provided by CNPq and Petrobras.

7. References

Adumitroaie, V., Ristorcelli, J., and Taulbee, D., 1998, Progress in Favre-Reynolds Stress Closures for Compressible Flows, Technical Report CR–2078423, NASA.

Figueira da Silva, L., Azevedo, J., and Korzenowski, H., 1999, On the Development of an Unstructured Grid Solver for Inert and Reactive High Speed Flow Simulations, "RBCM - Jornal of the Brazilian Society of Mechanical Sciences", Vol. XXI, No. 4, pp. 564–579.

Figueira da Silva, L., Azevedo, J., and Korzenowski, H., 2000, Unstructured Adaptive Grid Flow Simulations of Inert and Reactive Gas Mixtures, "Journal of Computational Physics", Vol. 160, No. 2, pp. 522–540.

Glassman, I., 1996, "Combustion", Academic Press, third edition.

Glaznev, V., 1991, Inverse Feedback Mechanism in Self-Oscillations in flow of an Underexpanded Supersonic Jet Against a Planar Obstacle, "Zhurnal Prikladnoi Mekhaniki i Tekhnicheskoi Fiziki (transl.)", Vol. , No. 4, pp. 59–63.

Gorshkov, G. and Uskov, V., 1999, Special Features of the Self-Sustained oscillations in a Supersonic Underexpanded Jet Impinging on an Obstacle with a Restricted Cross-Section, "Prikladnaya Mekhanika i Tekhicheskaya Fizika (transl.)", Vol. 40, No. 4, pp. 143–149.

Gorshkov, G., Uskov, V., and Favoriskii, V., 1993, Nonstationary Flow of an Underexpanded Jet around and Unbounded Obstacle, "Prikladnaya Mekhanika i Tekhicheskaya Fizika (transl.)", Vol. , No. 4, pp. 58–65.

Hirsch, C., 1990, "Numerical Computations of Internal and External Flows", Vol. 2, chapter 21, pp. 493–594. John Wiley & Sons, Inc., Chichester.

Kee, R. J., Dixon-Lewis, G., Warnatz, J., Coltrin, M. E., and Miller, J. A., 1986, A Fortran Computer Code Package for the Evaluation of Gas Phase Multicomponent Transport Properties, Technical Report SAND89-86246/UC-401, Sandia National Laboratories.

Kee, R. J., Rupley, F. M., and Miller, J. A., 1991, CHEMKIN-II: A Fortran Chemical Kinetics Package for the Analysis of Gas Phase Chemical Kinetics, Technical Report SAND89-8009B/UC-706, Sandia National Laboratories.

Liou, M.-S., 1996, A Sequel to AUSM: AUSM$^+$, "Journal of Computational Physics", Vol. 129, No. 2, pp. 364–382.

Mavriplis, D., 1988, Multigrid Solution of the Two-Dimensional Euler Equations on Unstructured Triangular Meshes, "AIAA Journal", Vol. 26, No. 7, pp. 824–831.

Panda, J., 1998, Shock Oscillation in Underexpanded Screeching Jets, "Journal of Fluid Mechanics", Vol. 363,

pp. 173–198.

Pimentel, C., Azevedo, J., Figueira da Silva, L., and Deshaies, B., 2002, Numerical Study of Wedge Supported Oblique Shock Wave-Oblique Detonation Wave Transitions, "Journal of the Brazilian Society of Mechanical Sciences", Vol. XXIV, No. 3, pp. 149–157.

Rauenzahn, R., 1986, "Analysis of Rock Mechanics and Gas Dynamics of Flame-Jet Thermal Spallation Drilling", PhD thesis, Massachussets Institute of Technology.

Rauenzahn, R. and Tester, J., 1991a, Numerical Simulation and Field Testing of Flame-Jet Thermal Spallation Drilling - 1. Model Development, "International Journal of Heat and Mass Trasnfer", Vol. 34, No. 3, pp. 795–808.

Rauenzahn, R. and Tester, J., 1991b, Numerical Simulation and Field Testing of Flame-Jet Thermal Spallation Drilling - 2. Experimental Verification, "International Journal of Heat and Mass Trasnfer", Vol. 34, No. 3, pp. 809–818.

Sakar, A. and So, R., 1997, A Critical Evaluation of Near-Wall Two-Equation Models Against Direct Numerical Simulation Data, "International Journal of Heat and Fluid Flow", Vol. 18, No. 2, pp. 197–208.

Sarkar, S., 1995, The Stabilizing Effect of Compressibility in Turbulent Shear Flow, "Journal of Fluid Mechanics", Vol. 282, pp. 163–186.

Sarkar, S., Erlebacher, G., Hussaini, M., and Kreiss, H., 1991a, The Analysis and Modelling of Dilatational Terms in Compressible Turbulence, "Journal of Fluid Mechanics", Vol. 227, pp. 473–493.

Sarkar, S., Erlebacher, G., and Hussaini, M. Y., 1991b, Direct Simulation of Compressible Turbulence in a Shear Flow, "Theoretical and Computational Fluid Dynamics", Vol. 2, pp. 291–305.

Shapiro, A., 1983, "The Dynamics and Thermodynamics of Compressible Fluid Flow", Robert E. Krieger Publishing Co., Malabar, Florida.

Sokolov, E., 1992, Breakdown of Steady Axisymmetric Flow in the Shock Layer Formed when a Supersonic Underexpanded Jet Interacts with a Perpendicular Flat Plate, "Izvestiya Rossiikoi Akademii Nauk, Mekhanika Zhidkisti i Gaza (transl.)", Vol. , No. 4, pp. 36–42.

Tester, J., Herzog, H., Chen, Z., Potter, R., and Frank, M., 1994, Prospects for Universal Geothermal Energy from Heat Mining, "Sciences & Global Security", Vol. 5, pp. 99–121.

Viegas, F., 2004, Perfuração de Rochas por Jato Supersônico Quente, Master's thesis, Instituto Nacional de Pesquisas Espaciais, Cachoeira Paulista.

Wilkinson, M., 1989, "Computational Modeling of the Gas-Phase Transport Phenomena and Experimental Investigation of Surface Temperatures During Flame-Jet Thermal Spallation Drilling", PhD thesis, Massachussets Institute of Technology.

Wilkinson, M. and Tester, J., 1993, Experimental Measurement of Surface Temperatures During Flame-Jet Thermal Spallation Drilling, "Rock Mechanics and Rock Engineering", Vol. 26, No. 1, pp. 29–62.

Williams, F. A., 1985, "Combustion Theory", Benjamin/Cummings Publishing Company, Inc., second edition.

Williams, R., Dey, T., Rauenzahn, R., Kranz, R., Tester, J., Potter, R., and Murphy, H., 1988, Advances in Thermal Spalltion Drilling Technology, Technical Report LA-11391-MS, Los Alamos National Laboratory.

Wu, P.-K., Mehrdad, S., Kierendall, K., and Nejad, A., 1999, Expansion and Mixing Processes of Underexpanded Supercritical Fuel Jets Injected into Superheated Conditions, "Journal of Propulsion and Power", Vol. 15, No. 5, pp. 642–649.

Zeman, O., 1993, A New Model for Super/Hypersonic Turbulent Boundary Layers, "31st Aerospace Sciences Meeting and Exhibit". American Institute of Aeronautics and Astronautics.

Zhang, H., So, R., Speziale, C., and Lai, Y., 1991, A Near-Wall Two-Equation Model for Compressible Turbulent Flows, Technical Report CR–1895565, NASA.